Bok, D., Basinger, S. F., and Hall, M. O. (1974), *Exp. Eye Res. 18,* 225.
Cohen, A. I. (1972), *in* Handbook of Sensory Physiology, Fuortes, M. G. F., Ed., West Berlin, Springer-Verlag, p 63.
Hall, M. O., and Bok, D. (1974), *Exp. Eye Res. 18,* 105.
Hall, M. O., Bok, D., and Bacharach, A. D. E. (1968), *Science 161,* 787.
Hall, M. O., Bok, D., and Bacharach, A. D. E. (1969), *J. Mol. Biol. 45,* 397.
Laico, M. T., Ruoslahti, E. I., Papermaster, D. S., and Dreyer, W. J. (1970), *Proc. Natl. Acad. Sci. U.S.A. 67,* 120.
Matsubara, T., Miyata, M., and Mizuno, K. (1968), *Vision Res. 8,* 1139.
O'Brien, P. J., and Muellenberg, C. G. (1973), *Arch. Biochem. Biophys. 158,* 36.
O'Brien, P. J., and Muellenberg, C. G. (1974), *Exp. Eye Res. 18,* 241.
O'Brien, P. J., Muellenberg, C. G., and Bungenberg de Jong, J. J. (1972), *Biochemistry 11,* 64.
Papermaster, D. S., and Dreyer, W. J. (1974), *Biochemistry 13,* 2438.
Shapiro, A. L., Viñuela, E., and Maizel, J. V. (1967), *Biochem. Biophys. Res. Commun. 28,* 815.
Shichi, H., and Somers, R. L. (1974), *J. Biol. Chem. 249,* 6570.
Wald, G. (1953), *Annu. Rev. Biochem. 22,* 497.
Young, R. W. (1971), *J. Cell Biol. 49,* 303.
Young, R. W., and Droz, B. (1968), *J. Cell Biol. 39,* 169.

Interaction of Effecting Ligands with *Lac* Repressor and Repressor–Operator Complex†

Mary D. Barkley,* Arthur D. Riggs,‡ Alan Jobe,# and Suzanne Bourgeois§

ABSTRACT: The equilibrium association constants for the binding of a wide variety of effecting ligands of the *lac* repressor were measured by equilibrium dialysis. Also, detailed investigations of the apparent rate of dissociation of repressor–operator complex as a function of ligand concentration were carried out for several inducers and anti-inducers. The affinity of repressor–ligand complex for operator DNA was evaluated from the specific rate constants at saturating concentrations of effecting ligand. By fitting the experimental data depicting the functional dependence of the rate of dissociation upon ligand concentrations to calculated curves, assuming simple models of the induction mechanism, the equilibrium association constant for the binding of effecting ligand to repressor–operator complex was determined. Inducers reduce the affinity of *lac* repressor for operator DNA by a factor of approximately 1000 under standard conditions; the extent of destabilization depends on Mg^{2+} ion concentration. Anti-inducers increase the affinity of repressor for operator at most a factor of five. Only one neutral ligand, which binds to repressor without altering the stability of repressor–operator complex, was found. No homotropic or heterotropic interactions in the binding of effecting ligands either to repressor or to repressor–operator complex are evident.

In the past 20 years, there have been a number of accounts of the specificity of induction of the lactose operon in *Escherichia coli.* The in vivo studies were primarily concerned with identifying effecting ligands of the *lac* repressor, the majority of which have turned out to be β-galactosides. In the first paper on this subject, Monod et al. (1951) investigated the effect of substitution of several functional groups at different positions on the galactose ring upon induction of the synthesis of β-galactosidase. Later systematic studies by Müller-Hill et al. (1964) and by Boos et al. (1967) enlarged the list of compounds examined, and classified a number of these sugars as inducers or anti-inducers of the operon. Müller-Hill et al. (1964) also attempted to describe those features of the sugar moiety which are important in making the molecule an effecting ligand, either inducing or anti-inducing. These studies with synthetic ligands yielded much valuable information; more recently, it has been demonstrated that allolactose is the natural inducer of the *lac* operon in vivo (Jobe and Bourgeois, 1972a).

With the isolation of the *lac* repressor protein, it became possible to study induction in vitro. The membrane filtration technique, using purified *lac* repressor and ^{32}P-labeled phage DNA bearing the *lac* operon, permitted examination of the effects of inducing and anti-inducing ligands upon the equilibrium and kinetic properties of the interaction of repressor protein and operator DNA. In the initial study of a few effecting ligands (Riggs et al., 1970b), the essential features of earlier experiments in vivo were verified. Compounds that were inducers or anti-inducers of β-galactosid-

† From the Salk Institute for Biological Studies, San Diego, California 92112, and the City of Hope National Medical Center, Duarte, California 91010. *Received October 30, 1974.* This research was supported by grants from the National Institutes of Health (GM20259, GM20868, HD04420) and the National Science Foundation (GB 29559 X, GB 26517).

*Recipient of a Postdoctoral Fellowship from the National Institutes of Health. Present address: Department of Chemistry, University of California—San Diego, La Jolla, California 92037.
‡ City of Hope National Medical Center, Duarte, California 91010.
§ Recipient of a Career Development Award from the National Institutes of Health.

Supported by a training grant the Institute of Allergy and Infectious Diseases to Dr. Melvin Cohn.

ase synthesis in vivo were shown to cause or prevent, respectively, disruption of repressor–operator complex in equilibrium experiments in vitro. Against this background, one purpose of this paper is to report the results of a comprehensive, quantitative investigation of a wide variety of effecting ligands of the *lac* repressor.

It was also demonstrated in kinetics experiments that the inducer isopropyl 1-thio-β-D-galactoside (IPTG)[1] increases the rate of dissociation of repressor–operator complex and the anti-inducer *o*-nitrophenyl β-D-fucoside (ONPF) decreases the rate of dissociation. Since neither IPTG (Jobe and Bourgeois, 1972b) nor ONPF (Lin and Riggs, 1972) alters the rate of association of repressor and operator DNA, the changes in the rate of dissociation may be ascribed directly to a decrease or increase in the affinity of repressor for operator in the presence of inducer or anti-inducer, respectively. These experiments established the existence of a ternary complex of ligand–repressor–operator by showing that effecting ligands interact with repressor–operator complex. Since kinetic effects are so important, a second purpose of this paper is to present a detailed study of the effect of IPTG on the rate of dissociation of repressor–operator complex.

We examine the binding of ligands by repressor protein from two aspects. We study the binding of ligand to free repressor protein, in order to measure the association constant for repressor and ligand and to ascertain whether there are any homotropic or heterotropic interactions upon binding of multiple ligands. We also look at the interaction of ligands with repressor bound to operator DNA, with the object of designating those ligands which bind to repressor protein as inducers or anti-inducers and of elucidating the mechanisms by which repressor–operator complex is disrupted or preserved by inducing or anti-inducing ligands, respectively. We compare the experimental data with sample calculations based on simple models for the induction process. By making certain assumptions, we predict the number of ligand molecules required for induction and determine the association constant for repressor–operator complex and ligand. The affinities of effecting ligands for free repressor and for repressor bound to operator are compared in order to inquire if the results are congruent with our notions about allosteric proteins.

Materials and Methods

Chemicals and Reagents

(*a*) *Sugars.* *p*-Aminophenyl 1-thio-β-D-galactoside, isopropyl 1-thio-β-D-galactoside, *o*-nitrophenyl β-D-galactoside, and *p*-nitrophenyl β-D-galactoside were purchased from Calbiochem. D-Fucose, galactose (glucose-free), *o*-nitrophenyl 1-thio-β-D-fucoside, *o*-nitrophenyl 1-thio-β-D-galactoside, *p*-nitrophenyl 1-thio-β-D-galactoside, and 2-phenylethyl β-D-galactoside were purchased from Cyclo Chemical Corporation. Glucose was purchased from Mallinckrodt. Methyl β-D-galactoside and methyl 1-thio-β-D-galactoside were purchased from Mann Research Laboratories. Lactose and melibiose were purchased from Pfanstiehl. *p*-Aminophenyl β-D-galactoside and 1,2,3,4,6-penta-*O*-acetyl-D-galactose were purchased from Pierce Chemical. *o*-Nitrophenyl β-D-fucoside, phenyl β-D-galactoside, and phenyl 1-thio-β-D-galactoside were purchased from Sigma Chemical Corporation.

[^{14}C]Isopropyl 1-thio-β-D-galactoside, 30 Ci/mol, was purchased from Calatomic. [^{14}C]Methyl 1-thio-β-D-galactoside, 2.2 Ci/mol, was purchased from New England Nuclear Corporation.

Thioallolactose (6-*S*-β-D-galactopyranosyl-6-thio-D-glucose) was a gift from W. Boos. Benzyl β-D-galactoside, benzyl 1-thio-β-D-galactoside, *n*-butyl β-D-galactoside, *n*-butyl 1-thio-β-D-galactoside, 2-phenylethyl 1-thio-β-D-galactoside, and *n*-propyl 1-thio-β-D-galactoside were gifts from M. Cohn. 6-Fluoro-6-deoxy-D-galactose was a gift from S. Opella.

Allolactose (6-*O*-β-D-galactopyranosyl-D-glucose) was synthesized as described before (Jobe and Bourgeois, 1972a). Isopropyl β-D-galactoside was synthesized as follows. 2,3,4,6-Tetra-*O*-acetyl-α-D-galactopyranosyl bromide was prepared by reacting 1,2,3,4,6-penta-*O*-acetyl-β-D-galactose and HBr (Hayes and Todd, 1950). The bromide was coupled to 2-propanol over Ag_2CO_3 (Helferich and Sparmberg, 1933). The product was deacetylated in methanol saturated with ammonium gas overnight (Davoll et al., 1948). Isopropyl β-D-galactoside was purified by column chromatography on silica gel with chloroform–methanol (4:1) eluate and recrystallization from ethyl acetate. The melting point is 123–123.5°. Anal. Calcd for $C_9H_{18}O_6$: C, 48.64; H, 8.16; O, 43.19. Found: C, 47.47; H, 8.58; O, 43.80. The mass spectrum is consistent with $C_9H_{18}O_6$. The identity of the compound was confirmed by paper chromatography, ir, and ^{1}H nuclear magnetic resonance using isopropyl 1-thio-β-D-galactoside and galactose for comparison.

(*b*) *Medium and Buffers.* Low phosphate medium is prepared as follows. After autoclaving 1 l. of DYT medium (16 g of Difco Bacto-tryptone, 10 g of Difco yeast extract, and 5 g of NaCl per l. of distilled water), add 10 ml of 1 *M* $MgSO_4$ and 6 ml of concentrated NH_4OH to the hot medium. Allow precipitate to form for several hours at 4°. Filter. Adjust pH to 7.4 with concentrated HCl. Sterilize by filtration.

Phage buffer (φ) is 0.02 *M* Tris-HCl (pH 7.4), 0.1 *M* NaCl, 1 m*M* $MgSO_4$, 0.1 m*M* dithiothreitol, and 50 μg/ml of bovine serum albumin.

Potassium phosphate buffer (KPB) is (KH_2PO_4, K_2HPO_4) of indicated molarity, pH 8.0, 1 m*M* dithioerythritol, and 1 m*M* sodium azide.

Standard binding buffer (BB) is 0.01 *M* Tris-HCl (pH 7.5), 0.01 *M* $Mg(CH_3CO_2)_2$, 0.01 *M* KCl, 0.1 m*M* EDTA, 0.1 m*M* dithioerythritol, 5% dimethyl sulfoxide, and 25 μg/ml of bovine serum albumin. The ionic strength of the standard BB is $I = 0.05$ *M*. The ionic strength, concentration of Mg^{2+}, and pH of BB are altered for some experiments, as indicated in the text. Filtering buffer (FB) is BB without dimethyl sulfoxide and bovine serum albumin.

(*c*) *Repressor Preparations.* Q repressor, used in most of the experiments, is isolated from the i^q strain BMH461: [*lac*pro]Δ (λh80CI857t68d*lac* $i^qz^+y^-$)/F′*lac* $i^qz^+y^-pro^+$ (Miller et al., 1968). Repressor protein was purified by ammonium sulfate fractionation, DNA-cellulose chromatography, and phosphocellulose chromatography. (Details of the purification scheme will be published elsewhere.) The purified protein forms a single band on analytical polyacrylamide gels. It is active with respect to operator binding, having a ratio of IPTG-binding sites to DNA-binding sites of about 4.

X86 repressor is isolated from the strain P90-86^q: [*lac*-

[1] Abbreviations used are: IPTG, isopropyl 1-thio-β-D-galactoside; ONPF, *o*-nitrophenyl β-D-fucoside; ONPG, *o*-nitrophenyl β-D-galactoside; TMG, methyl 1-thio-β-D-galactoside.

pro]Δ (λh80CI857t68d*lac* $i^{X86q}z^+$)/F′*lac* $i^{X86}z^+pro^+$ (J. Miller, see Jobe and Bourgeois, 1972b). The repressor was purified by ammonium sulfate fractionation, DNA-cellulose chromatography, and DEAE-cellulose chromatography.

(*d*) *DNA Preparations.* ^{32}P-labeled λϕ80 d*lac* DNA is isolated from the double lysogen RV80: [*lac*]ΔX74 (λh80CI857t68/λh80CI857t68d*lac*) (M. Malamy). The procedure used was similar to that described before (Lin and Riggs, 1972) with the modification that the cells were grown on low phosphate medium to A_{600} = 1.8 at 30° prior to heat induction.

Unlabeled λϕ80 d*lac* DNA is prepared as described above, with the exceptions that the cells were grown on DYT and the equilibrium CsCl gradient was omitted. The solution of unlabeled viral DNA contains a mixture of ϕ80 and ϕ80 d*lac* DNAs in approximately equal concentrations.

^{32}P-labeled λp*lac*5 DNA is isolated from the single lysogen G141: [*lac*]Δ U169 B_1^-(λCI857S7p*lac*5 $i^-z^+y^-$) (W. Gilbert). Cells were grown on low phosphate medium supplemented with 0.4% glucose at 32° to a cell density corresponding to A_{600} = 0.5. Phage multiplication was induced at 45° for 10 min; 10 μCi of carrier-free [^{32}P]phosphate/ml was added, and the culture was incubated at 37° for 4 hr. Cells were harvested, suspended in 1/5 the volume of ϕ buffer, lysed with chloroform, treated with 1 μg of DNase/ml at 37° for 10 min, and left overnight at 5°. Another 0.5 μg of DNase/ml was added with gentle stirring at 5° for 10 min. The aqueous layer was decanted, and the cell debris and any traces of chloroform were removed from the lysate by sedimentation. The phage were pelleted in the ultracentrifuge, then suspended in ϕ buffer with gentle stirring at 5° overnight; the resulting suspension was clarified by sedimentation. This step was repeated once. Viral DNA was purified from the phage by extraction with phenol, dialyzed against 0.01 *M* Tris-HCl (pH 7.4), 1 m*M* EDTA, and 1% v/v ethanol, and stored at 5° over chloroform.

Unlabeled λp*lac*5 DNA is prepared by the method of Zubay (1973).

Experimental Procedures

(*a*) *Equilibrium dialysis* is carried out in microdialysis chambers (purchased from Gateway Immunosera Company, Cahokia, Ill.). In the usual dialysis experiment, 0.1 ml of Q repressor solution in 0.1 *M* KPB is introduced on one side of the membrane and 0.1 ml of ligand solution in 0.1 *M* KPB on the other side. The dialysis cells are attached to a slowly revolving platform, and rotated at 4° for 10–12 hr, at an angle of inclination such that the air bubble in the cell moves around the chamber during the course of one revolution. (Under these conditions, equilibration of sugar molecules across the membrane is achieved within 5 hr.) At the end of this time, 50-μl aliquots are removed from each side of the dialysis membrane and counted in a liquid scintillation counter. For experiments with repressor concentrations <100 μg/ml, 100 μg/ml of bovine serum albumin is added to the repressor solution to prevent loss of repressor protein during dialysis.

For determination of the association constant of a labeled ligand, repressor concentration was fixed and the concentration of radioactive ligand varied in a given experiment. The data were plotted according to Scatchard (1949). At present, because of a limitation in the repressor concentrations attainable, association constants $<10^4\ M^{-1}$ cannot be measured directly by binding of labeled ligand to repressor. In order to measure equilibrium constants for the binding of ligands which are not radioactively labeled or which have low affinity for repressor, competition of the binding of [^{14}C]IPTG by the unlabeled ligand was followed in equilibrium dialysis experiments. The association constant for the unlabeled ligand, when present in large excess of the repressor concentration, was determined from a double reciprocal plot of the data (Lineweaver and Burk, 1934). Otherwise, it was determined from the data at 50% competition.

(*b*) *Equilibrium Dissociation of Repressor–Operator Complex.* The use of membrane filtration to monitor the binding of *lac* repressor protein and operator DNA has been described (Riggs et al., 1970c). Experiments to test the effect of inducing ligands on the repressor–operator binding equilibrium as a function of the concentration of inducer were done as before (Riggs et al., 1970b) with the following modifications. 2×10^{-12} *M* ^{32}P-labeled d*lac* DNA (based on a molecular weight of 3×10^7 for λ DNA) and a saturating amount of Q repressor were equilibrated in BB in the presence of various concentrations of inducer. Three 0.5-ml aliquots of each sample were filtered on Millipore filters (Type HA, 24 mm); the filters were washed with 0.5 ml of FB. Background was determined from a sample containing 1.25 m*M* IPTG. Triplicate filter bound counts for a 1000-fold range of ligand concentrations were obtained, averaged, corrected for background, and plotted on semilog paper. The inducer concentration at which the filter bound counts are reduced to one-half the value in the absence of inducer was read from the graph; this concentration is called κ.

(*c*) *Kinetics of Dissociation of Repressor–Operator Complex.* Because retention of repressor–operator complex by membrane filters is essentially eliminated at relatively high concentrations of inducer, the rapid rates of dissociation corresponding to half-lives <1 min cannot be measured without taking some precautions. We were able to overcome this problem using the following experimental regime. 6.66×10^{-11} *M* ^{32}P-labeled p*lac* DNA and 1.43×10^{-10} *M* Q repressor were mixed in 3.5 ml of BB. After 10 min or more to reach equilibrium, 30 μl of this ^{32}P-labeled repressor–operator complex was placed in a plastic tube. At time zero, 0.3 ml of release solution, containing the desired buffer and concentration of inducer, and also 20 μg/ml of unlabeled p*lac* DNA, was added to the tube with rapid mixing. At time *t*, 0.6 ml of stop solution, BB′ (3 m*M* Mg^{2+}) containing 0.5 *M* glucose and 5 m*M* ONPF, both compounds being anti-inducers, was added with rapid mixing. Precisely 30 sec after adding stop solution, a 0.5-ml sample was filtered; the filter was washed with 0.5 ml of FB′ (3 m*M* Mg^{2+}). Background was the filter bound counts remaining after 10 min or more exposure to 1 m*M* IPTG. At each concentration of inducer, filter bound counts for several dissociation times were obtained, corrected for background, and plotted on semilog paper; the apparent specific rate constant of dissociation was calculated from the slope of the line. Using this procedure, where anti-inducers are used to stop the reaction and restore the filter retention of remaining ^{32}P-labeled repressor–operator complexes, half-lives as short as 5 sec can be measured accurately.

The rate of dissociation of repressor–operator complex for X86 repressor in the presence of inducing ligand was measured as before (Jobe and Bourgeois, 1972b) with minor modifications. 2×10^{-12} *M* ^{32}P-labeled d*lac* DNA was equilibrated with a saturating amount of X86 repressor in BB containing 2 μg/ml of chicken blood DNA. At time

Table I: Equilibrium Binding Data.

	K_2 (M^{-1})[a]	κ (M)	κK_2
Inducers			
Methyl β-D-galactoside	$(1.0 \pm 0.1) \times 10^4$	7×10^{-4}	7.0
Methyl 1-thio-β-D-galactoside	1.1×10^5	5×10^{-5}	5.6
n-Propyl 1-thio-β-D-galactoside	$(1.3 \pm 0.1) \times 10^6$	3.5×10^{-6}	4.6
Isopropyl β-D-galactoside	$(9.9 \pm 1.5) \times 10^3$	2×10^{-4}	1.9
Isopropyl 1-thio-β-D-galactoside	$(1.2 \pm 0.2) \times 10^6$	5×10^{-6}	6.2
n-Butyl β-D-galactoside	$(1.1 \pm 0.2) \times 10^5$	4×10^{-5}	4.5
n-Butyl 1-thio-β-D-galactoside	$(2.0 \pm 0.2) \times 10^5$	1×10^{-5}	2.0
Benzyl β-D-galactoside	$(1.04 \pm 0.02) \times 10^3$		
Benzyl 1-thio-β-D-galactoside	$(2.3 \pm 0.1) \times 10^3$	2.2×10^{-3}	2.5
2-Phenylethyl β-D-galactoside	$(5.1 \pm 0.1) \times 10^3$	8×10^{-4}	3.2
2-Phenylethyl 1-thio-β-D-galactoside	$(7.8 \pm 2.4) \times 10^2$	2.4×10^{-3}	1.8
p-Aminophenyl β-D-galactoside	$(5.23 \pm 0.05) \times 10^2$	2.8×10^{-3}	1.5
p-Aminophenyl 1-thio-β-D-galactoside	$(7.6 \pm 1.7) \times 10^2$	1×10^{-3}	0.8
o-Nitrophenyl 1-thio-β-D-galactoside	$(3.6 \pm 0.6) \times 10^2$	5.4×10^{-3}	1.9
p-Nitrophenyl β-D-galactoside	$(4.3 \pm 0.2) \times 10^2$	4.7×10^{-3}	2.0
p-Nitrophenyl 1-thio-β-D-galactoside	$(2.4 \pm 0.9) \times 10$	1.8×10^{-2}	0.4
D-Fucose	$(2.2 \pm 0.3) \times 10^2$	2.5×10^{-2}	5.6
Galactose	$(9.9 \pm 1.0) \times 10^2$	3×10^{-3}	3.0
6-Fluoro-6-deoxy-D-galactose		5.5×10^{-3}	
Melibiose (6-*O*-α-D-galactopyranosyl-D-glucose)	$(9.7 \pm 1.7) \times 10^3$	4.2×10^{-4}	4.2
Allolactose (6-*O*-β-D-galactopyranosyl-D-glucose)	$(1.7 \pm 0.2) \times 10^6$	5×10^{-6}	8.3
Thioallolactose (6-*S*-β-D-galactopyranosyl-D-glucose)	$(3.3 \pm 0.1) \times 10^5$	2.5×10^{-5}	8.1
Neutral			
o-Nitrophenyl β-D-galactoside	$(9.2 \pm 1.5) \times 10^3$		
Anti-inducers			
Phenyl β-D-galactoside	$(1.1 \pm 0.3) \times 10^3$		
Phenyl 1-thio-β-D-galactoside	$(2.3 \pm 0.1) \times 10^2$		
o-Nitrophenyl β-D-fucoside	$(7.1 \pm 2.7) \times 10^3$		
o-Nitrophenyl 1-thio-β-D-fucoside	$(1.48 \pm 0.00) \times 10^2$		
Glucose	$(1.4 \pm 0.2) \times 10$		
Lactose (4-*O*-β-D-galactopyranosyl-D-glucose)	3.0 ± 1.2		

[a] Each value is the average of two or more measurements.

zero, a 50-fold excess of unlabeled d*lac* DNA and inducing ligand to yield a given final concentration were added, and the solution was mixed briefly. At various times, a 1-ml aliquot was removed and added to 0.6 ml of stop solution, BB containing 0.01 *M* ONPF, with rapid mixing. Three 0.5-ml aliquots were filtered immediately; the filters were washed with 0.5 ml of FB. Background was determined separately by mixing the ^{32}P-labeled and unlabeled DNAs prior to addition of repressor.

The rate of dissociation of repressor–operator complex for Q repressor in the presence of anti-inducing ligands was determined as described previously (Jobe and Bourgeois, 1973) except that unlabeled d*lac* DNA was added in 50-fold excess over ^{32}P-labeled d*lac* DNA, and background was measured as described above. A control sample without anti-inducing ligand was run for each experiment.

Results

The simplest scheme describing the interactions of *lac* repressor protein (R), operator DNA (O), and effecting ligand (L), with which our data may be reconciled is

$$\begin{array}{ccc} R + O & \overset{{}^0k_{f1}}{\underset{{}^0k_{b1}}{\rightleftharpoons}} & RO \\ + & & + \\ L & & L \\ \Big\updownarrow K_2 & & \Big\updownarrow K_3 \\ RL + O & \underset{k_{b1}}{\overset{k_{f1}}{\rightleftharpoons}} & ORL \end{array}$$

where ${}^0k_{f1}$ and ${}^0k_{b1}$ are the specific rate constants of association and dissociation, respectively, for the binding of repressor and operator; and k_{f1} and k_{b1} are the specific rate constants of association and dissociation, respectively, for the binding of repressor–ligand complex and operator. The equilibrium association constants for these reactions are

$${}^0K_1 = \frac{{}^0k_{f1}}{{}^0k_{b1}} = \frac{[RO]}{[R][O]} \quad (1.0)$$

$$K_1 = \frac{k_{f1}}{k_{b1}} = \frac{[ORL]}{[RL][O]} \quad (1.1)$$

$$K_2 = \frac{[RL]}{[R][L]} \quad (2)$$

$$K_3 = \frac{[ORL]}{[RO][L]} \quad (3)$$

More complex models are presented in the Appendix.

Inducers

(*a*) *Equilibrium Binding.* The association constants K_2 for the binding of inducing ligand to *lac* repressor as determined by equilibrium dialysis are given in the first column of Table I. For the two inducers of sufficiently high affinity, which are available in radioactive form, ^{14}C-labeled IPTG and methyl 1-thio-β-D-galactoside (TMG), the association constants were determined from Scatchard plots (not shown) of the equilibrium dialysis data. In both cases, the Scatchard plots were linear, indicating that the inducer binding sites of the repressor behave as identical, independent sites. The equilibrium constants for the binding of unlabeled inducers to repressor were determined by competition of the binding of [^{14}C]IPTG. In all cases where the equilibrium dialysis data were treated according to Line-

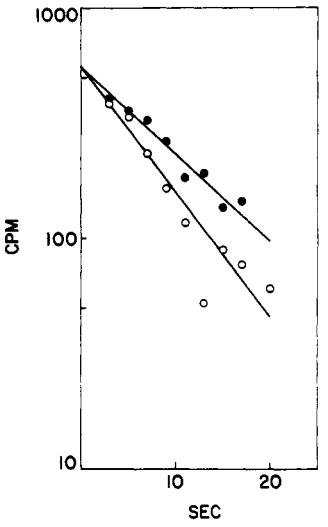

FIGURE 1: Rates of dissociation of IPTG-repressor-operator complex. (●) 2×10^{-4} *M* IPTG, $t_{1/2}$ = 8 sec, $k_{bapp} = 8.67 \times 10^{-2}$ sec^{-1}. (○) 3×10^{-4} *M* IPTG, $t_{1/2}$ = 5.5 sec, $k_{bapp} = 1.25 \times 10^{-1}$ sec^{-1}. The line is a least-squares fit of the data; the slope of this line equals k_{bapp}.

weaver and Burk, the double reciprocal plots (not shown) were linear; the intercept on the ordinate remained constant, indicating that the unlabeled inducers are competitive inhibitors of the [^{14}C]IPTG binding.

The values of κ, the molarity of inducer required for one-half inhibition of the equilibrium binding of repressor protein and operator DNA (see Materials and Methods, and Riggs et al., 1970b), are presented in the second column of Table I. It should be emphasized that κ is merely a convenient empirical constant. Theoretically, it would be related to the affinity of inducing ligand for repressor-operator complex by a complicated quadratic expression, obtained by simultaneous solution of eq 1.0, 2, and 3 and the accompanying conservation constraints. But in practice, since dissociation of repressor-operator complex by inducer occurs on membrane filters (Bourgeois and Riggs, 1970), and since the efficiency of retention of repressor-operator complex by the filters varies with ligand concentration, more elegant quantitative treatment of the data are not justified. Despite the ambiguity in interpretation, the assay is a simple, qualitative test for categorizing ligands as inducers based on their effect on the repressor-operator binding equilibrium. Also at constant filtration rate, the value of κ obtained for a given inducer is reproducible, and the sigmoidal shape of the semilog plot is the same for all inducers. κ may be considered as a functional measure of the relative effectiveness of inducing ligands. The potency of an inducer is roughly proportional to its affinity for free repressor as demonstrated in the last column of Table I, where the ratio of the association constant K_2 to $1/\kappa$ is tabulated.

(*b*) *Effect of IPTG on the Rate of Dissociation of Repressor-Operator Complex.* A detailed investigation of the dependence of the specific rate constant for dissociation of repressor-operator complex upon the concentration of inducing ligand has been carried out for the inducer IPTG. As demonstrated in Figure 1, the rate of dissociation of repressor-operator complex can be measured accurately by the membrane filter assay, even at high concentrations of inducer where the half-lives are as short as 5 sec, using the procedure described under Materials and Methods. Figure 2a shows a plot of the apparent specific rate constant of dissociation k_{bapp} vs. IPTG concentration; the closed circles

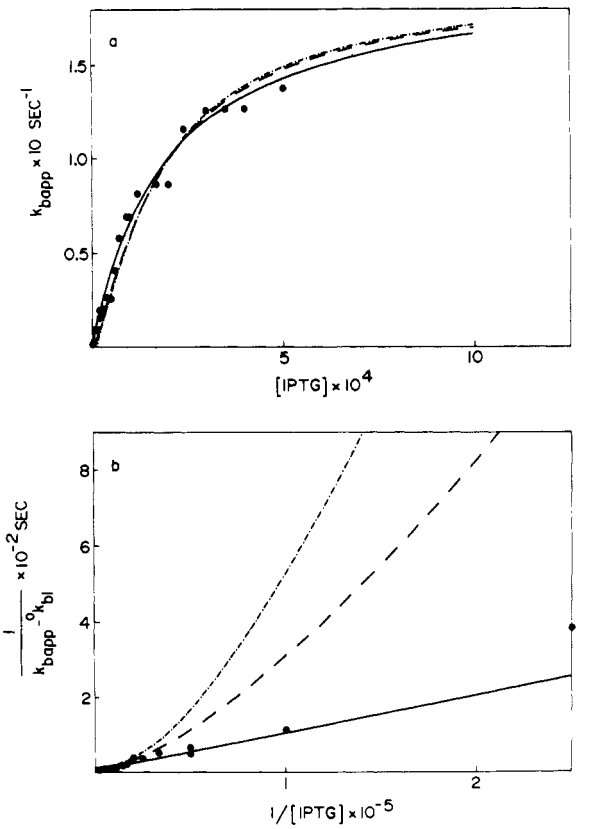

FIGURE 2: Dependence of apparent rate constant of dissociation upon IPTG concentration. (●) Data from kinetics experiments, as shown in Figure 1. Theoretical curves for the noncooperative model are fit to the data. (—) N = 1. (- -) N = 2. (· - ·) N = 4. (a) Plot of k_{bapp} vs. [IPTG]. (b) Double reciprocal plot of $1/(k_{bapp} - {}^0k_{bl})$ vs. $1/$[IPTG]. The intercept on the ordinate equals $1/(k_{bl} - {}^0k_{bl})$. The slope of the solid line equals $1/K_3(k_{bl} - {}^0k_{bl})$.

are the data points from a series of individual experiments similar to those depicted in Figure 1. There are three features to be noted in reference to this curve. First, at high concentrations of IPTG, the apparent rate constant approaches a limiting value, at which point the sites for inducer on repressor protein bound to operator are saturated with IPTG and there can be no further change in the apparent rate constant. Second, the curve of k_{bapp} vs. IPTG is hyperbolic. And third, the affinity of ligand for repressor-operator complex is determined from these experiments. The mathematical basis for the analysis of the kinetics data is developed in the Appendix, and the interpretation of the experimental data is presented below.

(i) EFFECTED RATE CONSTANT k_{bl}. At high IPTG concentrations, the apparent specific rate constant becomes independent of concentration of inducer, the value of the rate constant at saturation being called the effected rate constant k_{bl}. Since accurate measurement of the small time constants for dissociation of repressor-operator complex at high inducer concentrations is difficult using the membrane filtration technique, the effected rate constant is best determined by extrapolation from a double reciprocal plot of the data of Figure 2. It is demonstrated in the Appendix that a plot of $1/(k_{bapp} - {}^0k_{bl})$ as an inverse function of the concentration of effecting ligand L, where ${}^0k_{bl}$ is the spontaneous specific rate constant of dissociation of repressor-operator complex in the absence of ligand, has an intercept on the ordinate of $1/(k_{bl} - {}^0k_{bl})$. Figure 2b contains a plot of $1/(k_{bapp} - {}^0k_{bl})$ vs. $1/$[IPTG]; the closed circles are the

experimental points. The value of $k_{bl} = 0.2$ sec^{-1} is computed for IPTG. The equilibrium association constant K_1 for the binding of repressor-IPTG complex to operator DNA can be calculated as the ratio of two rate constants. Knowing that the specific rate constant of association of repressor and operator ${}^0k_{fl}$ is not altered by the presence of effecting ligands, under standard conditions

$$K_1 = \frac{{}^0k_{fl}}{k_{bl}} = \frac{7 \times 10^9\ M^{-1}\ \text{sec}^{-1}}{0.2\ \text{sec}^{-1}} = 3.5 \times 10^{10}\ M^{-1}$$

The affinity of repressor protein for operator DNA is decreased about 1000-fold from ${}^0K_1 = 3.5 \times 10^{13}\ M^{-1}$ in the absence of effecting ligand to $K_1 = 3.5 \times 10^{10}\ M^{-1}$ in the presence of saturating amounts of IPTG.

(ii) MODELS OF THE INDUCTION MECHANISM. The mathematical features of two simple models of induction, the extreme cooperative model and the noncooperative model, are derived in the Appendix. The extreme cooperative model assumes that binding of a given inducer molecule to repressor-operator complex causes a concerted allosteric transformation in the repressor tetramer; decomposition of the ternary complex to repressor-IPTG complex and free operator DNA switches from a kinetic process governed by the spontaneous rate constant ${}^0k_{bl}$ to one governed by the effected rate constant k_{bl}. This mechanism requires strong cooperation between the N sites for ligand on repressor bound to operator and predicts a pronounced sigmoidal dependence of k_{bapp} on inducer concentration, if any molecule other than the ultimate triggers the conformational change. If the Nth ligand bound induces, the curve of k_{bapp} vs. [IPTG] is hyperbolic and indistinguishable from the situation in which there is only one low-affinity site for inducer on repressor-operator complex. Alternatively, the noncooperative model presumes that each subunit of the repressor tetramer which interacts with operator may be induced independently. Binding of an inducer molecule to repressor-operator complex causes an alteration in the conformation of the subunit to which it binds, weakening the interaction of that repressor subunit with operator; full induction is achieved when repressor-operator complex is saturated with ligand. The prediction based on this mechanism is that a plot of k_{bapp} vs. [IPTG] be hyperbolic, or approximately so. Slight curvature may be evidenced at low concentrations of inducer, the degree depending on the number of repressor subunits N interacting with operator.

Since the plot of k_{bapp} vs. [IPTG] is hyperbolic, the highly cooperative models with positive interactions between inducer sites can be excluded immediately. In order to compare the experimental data with the theoretical curves, measured values of ${}^0k_{bl}$ and k_{bl} are substituted into eq 20 of the Appendix, and the resulting curve of k_{bapp} vs. $X = K_3[L]$ is fitted to the plot of k_{bapp} vs. [IPTG]. K_3 is chosen such that the midpoints of the calculated and experimental curves coincide. Figure 2a shows several curves for the noncooperative model with different values of N, where each repressor subunit contributes equally to the interaction with operator and the inducer sites on repressor-operator complex are identical and independent: the solid line is $N = 1$, $K_3 = 5.0 \times 10^3\ M^{-1}$, the broken line is $N = 2$, $K_3 = 1.1 \times 10^4\ M^{-1}$, and the dotted line is $N = 4$, $K_3 = 2.1 \times 10^4\ M^{-1}$. In principle, we could distinguish between the cases of $N = 1$ and $N > 1$ from the shape of the double reciprocal plot of the data at larger values of 1/[IPTG]. Plots of $1/(k_{bapp} - {}^0k_{bl})$ vs. 1/[IPTG] for the data points and calculated curves of Figure 2a are presented in Figure 2b. Although slight curvature at low concentrations of IPTG cannot be excluded, the data fit best for $N = 1$. We conclude that the experimental data for k_{bapp} as a function of IPTG concentration are most simply rectified by a scheme in which repressor protein bound to operator has one apparent site for IPTG.

(iii) EQUILIBRIUM ASSOCIATION CONSTANT K_3. In membrane filtration experiments, we measure an apparent affinity for the binding of effecting ligand to repressor-operator complex. This affinity is proportional to the true value, the factor depending on the number of sites $N = 1, \ldots, 4$ for inducer on repressor bound to operator DNA. The equilibrium association constant K_3 for the binding of IPTG to repressor-operator complex is determined from the functional dependence of k_{bapp} on IPTG concentration by straightforward graphical procedures (see Appendix). K_3 is computed either from the plot of k_{bapp} vs. [L] as $K_3 = 1/L^0$, where L^0 is the concentration of effecting ligand causing half the change in the apparent specific rate constant k_{bapp} from the spontaneous rate constant ${}^0k_{bl}$ in the absence of ligand to the effected rate constant k_{bl} at saturating concentrations of ligand, or from the double reciprocal plot of $1/(k_{bapp} - {}^0k_{bl})$ vs. 1/[L], which has a slope of $1/K_3(k_{bl} - {}^0k_{bl})$. In the following presentation of results, we employ this apparent equilibrium association constant, keeping in mind that the true equilibrium constant may differ from K_3 by as much as a factor of five. Note that this method of calculating K_3 is equivalent to assuming $N = 1$.

(*c*) *Effect of Reaction Conditions on* k_{bl} *and* K_3. The dependence of k_{bapp} upon IPTG concentration was also studied as a function of ionic strength, Mg^{2+} ion concentration, pH, and temperature. For each condition, several kinetics experiments were done at various concentrations of IPTG. The apparent rate constants of dissociation were calculated and plotted in double reciprocal fashion. In all cases, the plots were linear. Two parameters, the effected rate constant k_{bl} and the association constant K_3 for the binding of ligand to repressor-operator complex, were obtained from the intercept and slope of these plots; the values of k_{bl} and K_3 are summarized in the first two columns of Table II. The effects of experimental conditions upon the ternary complex, IPTG-repressor-operator, are discussed below in terms of these constants. To facilitate interpretation, data for the dependence upon ionic strength (I) of the specific rate constants for association ${}^0k_{fl}$ and dissociation ${}^0k_{bl}$ and of the equilibrium association constant ${}^0K_1$, for the binding of repressor to operator DNA in the absence of effecting ligand, are included in Table II, along with control values for ${}^0k_{bl}$ at different Mg^{2+} ion concentrations, pH's, and temperatures. In those situations where the rate constant of association k_{fl} at saturating concentrations of effecting ligand could be measured (using X86 repressor in experiments with IPTG, Jobe and Bourgeois, 1972b, and Q repressor with ONPF, Lin and Riggs, 1972), no change in the rate of association was detected. These results are generalized to assert that the rate constant of association of Q repressor and operator is not effected by IPTG. Thus, the equilibrium association constants K_1 for the binding of repressor-IPTG complex to operator may be computed, and are given in the last column of Table II.

(i) IONIC STRENGTH. The effected rate constant of dissociation k_{bl} increases with ionic strength. The semilog plots (not shown) of ${}^0K_1$ and K_1 vs. $[I]^{1/2}$ are linear and have equal slopes, suggesting that the decrease in the affinity of repressor for operator with increasing ionic strength is

Table II: Kinetic Studies of the Effect of Reaction Conditions upon the IPTG–Repressor–Operator Interaction.

	k_{b1} (sec^{-1})[a]	K_3 (M^{-1})[a]	${}^0k_{f1}$ (M^{-1} sec^{-1})[b]	${}^0k_{b1}$ (sec^{-1})[a]	${}^0K_1$ (M^{-1})	K_1 (M^{-1})
			Ionic Strength Varied: $[Mg^{2+}] = 3 \times 10^{-3} M$			
I (M)						[c]
0.02	$(1.9 \pm 0.1) \times 10^{-2}$	$(1.42 \pm 0.2) \times 10^4$	5.8×10^9[d]			3.1×10^{11}
0.03	$(3.1 \pm 0.1) \times 10^{-2}$	$(1.0 \pm 0.1) \times 10^4$	5.3×10^9	$(1.8 \pm 0.2) \times 10^{-4}$	2.9×10^{13}	1.7×10^{11}
0.05	$(4.0 \pm 0.4) \times 10^{-2}$	$(1.3 \pm 0.2) \times 10^4$	2.7×10^9	1.9×10^{-4}	1.4×10^{13}	6.7×10^{10}
0.08					5.7×10^{12}	
0.10	$(1.15 \pm 0.06) \times 10^{-1}$	$(6.3 \pm 0.4) \times 10^3$	1.74×10^9	6.1×10^{-4}	2.9×10^{12}	1.5×10^{10}
0.15			1.1×10^9	1.15×10^{-3}	9.5×10^{11}	
0.16	$(2.4 \pm 0.7) \times 10^{-1}$	$(1.7 \pm 0.8) \times 10^4$	7.6×10^8[d]			3.2×10^9
0.20			4.3×10^8	$(1.5 \pm 0.1) \times 10^{-3}$	2.9×10^{11}	
			Magnesium Ion Varied: $I = 0.05 M$			
$[Mg^{2+}]$ (M)						[e]
0	$(1 \pm 0.1) \times 10^{-3}$	$(2.9 \pm 0.8) \times 10^5$		$(1.8 \pm 0.2) \times 10^{-4}$		2.7×10^{12}
0.0010	$(5 \pm 0.5) \times 10^{-3}$	$(1.7 \pm 0.1) \times 10^5$				5.4×10^{11}
0.0015	$(9 \pm 0.4) \times 10^{-3}$	$(8.2 \pm 0.7) \times 10^4$				3.0×10^{11}
0.003	$(4 \pm 0.4) \times 10^{-2}$	$(1.3 \pm 0.2) \times 10^4$	2.7×10^9			6.7×10^{10}
0.006	$(1.3 \pm 0.4) \times 10^{-1}$	$(5.0 \pm 1.7) \times 10^3$				2.1×10^{10}
0.010	$(2.0 \pm 0.4) \times 10^{-1}$	$(5.0 \pm 1.3) \times 10^3$	2×10^9	$(1.9 \pm 0.2) \times 10^{-4}$		1.3×10^{10}
			pH Varied: $[Mg^{2+}] = 1 \times 10^{-2} M$, $I = 0.05 M$			
pH						
7.0	$(1.1 \pm 0.1) \times 10^{-1}$	$(1.1 \pm 0.1) \times 10^4$				
7.2	$(2.1 \pm 0.6) \times 10^{-1}$	$(4.0 \pm 1.4) \times 10^3$				
7.4	$(2.0 \pm 0.4) \times 10^{-1}$	$(5.0 \pm 1.3) \times 10^3$		$(1.9 \pm 0.2) \times 10^{-4}$		
7.8	$(3.5 \pm 0.6) \times 10^{-1}$	$(2.8 \pm 0.5) \times 10^3$				
8.0	$(1.5 \pm 0.3) \times 10^{-1}$	$(4.2 \pm 1.2) \times 10^3$		2.3×10^{-4}		
8.4	$(2.7 \pm 1.0) \times 10^{-1}$	$(2 \pm 0.8) \times 10^3$				
8.6				3.3×10^{-4}		
			Temperature Varied: $[Mg^{2+}] = 1 \times 10^{-2} M$, $I = 0.05 M$			
Temp (°C)						
0	$(1.2 \pm 0.3) \times 10^{-1}$	$(7.1 \pm 2.5) \times 10^3$		1.4×10^{-4}		
25	$(2.0 \pm 0.4) \times 10^{-1}$	$(5.0 \pm 1.3) \times 10^3$		2×10^{-4}		
37				3.5×10^{-4}		

[a] Values calculated by linear regression of the data to 70% confidence. [b] ${}^0k_{f1}$ calculated from ${}^0k_{f1} = {}^0K_1 {}^0k_{b1}$. [c] K_1 calculated from $K_1 = {}^0k_{f1}/k_{b1}$, since $k_{f1} = {}^0k_{f1}$. [d] Value determined graphically from linear plot of log ${}^0k_{f1}$ vs. $I^{1/2}$. [e] K_1 calculated from $K_1 = {}^0k_{f1}/k_{b1}$, presuming ${}^0k_{f1}$ is independent of $[Mg^{2+}]$.

the same in the presence or absence of IPTG. K_3 is independent of ionic strength.

(ii) MAGNESIUM ION CONCENTRATION. Since the rate constant for dissociation ${}^0k_{b1}$ of repressor–operator complex in the absence of IPTG does not depend on Mg^{2+} ion concentration, the large changes observed in k_{b1} and K_3 reflect specific effects of magnesium on the induction phenomenon. Assuming that the rate constant of association ${}^0k_{f1}$ is also independent of Mg^{2+} ion concentration, K_1 is calculated. At constant ionic strength, increasing Mg^{2+} from 0 to 0.01 M causes a 200-fold decrease in the binding constant K_1 of repressor–IPTG complex to operator and a 50-fold decrease in the apparent binding constant K_3 of IPTG to repressor–operator complex; in the absence of Mg^{2+}, the ternary complex is maximally stable.

(iii) pH. Both the spontaneous and effected rate constants of dissociation, ${}^0k_{b1}$ and k_{b1}, are insensitive to changes in pH from 7.0 to 8.6, as seen in Table II. For a wild-type repressor from strain E203, the rate constant of association in the absence of inducer, ${}^0k_{f1}$, and thus also the equilibrium association constant ${}^0K_1$, decreased by a factor of four over this pH range (Riggs et al., 1970a). We surmise that the association constant of repressor–IPTG complex and operator DNA, K_1, would have a similar dependence on pH. K_3 decreases slightly from pH 7.0 to 8.4, but the scatter in the data makes the trend at best marginal.

(iv) TEMPERATURE. The effected rate constant of dissociation k_{b1} shows a small increase, proportional to that observed for the spontaneous rate constant of dissociation ${}^0k_{b1}$, with increasing temperature from 0 to 25°. K_3 remains constant within experimental error over this temperature range.

In short, changes in ionic strength, pH, and temperature have no effects on the stability of IPTG–repressor–operator complex beyond those observed for repressor–operator complex. The affinity of IPTG for repressor–operator complex is also not altered by changes in these variables. On the other hand, Mg^{2+} ion concentration influences drastically both the stability of the ternary complex and the affinity of IPTG for repressor bound to operator, while not affecting the interaction of repressor and operator.

(*d*) *Kinetic Studies with Other Inducers.* The effects of a few inducing ligands on the apparent rate constant of dissociation were characterized and the results are collected in Table III. In experiments identical with those already described for IPTG, the dependence of k_{bapp} on concentration of inducer was determined for TMG and melibiose. Values for the effected rate constant of dissociation k_{b1} and the apparent equilibrium association constant K_3 for the binding of inducer to repressor–operator complex were obtained from the intercept and slope of the linear double reciprocal plots and are given in Table III, column 1. The ratios of the association constant K_2 for the binding of inducer to repressor, as measured by equilibrium dialysis, to K_3 are also tabulated in column 1. There are two immediate points to be noted. Namely, that within experimental error, for the three inducers which have been examined in detail, k_{b1} is the same. Also, these three inducing ligands have approximate-

Table III: Summary of Equilibrium and Kinetics Data.

	1. Q Repressor					2. X-86 Repressor
	$^0k_{b1}$ (sec^{-1})[a]	k_{b1} (sec^{-1})[a]	K_3 (M^{-1})[a]	K_2/K_3	$^0K_1/K_1$	k_{b1} (sec^{-1})[a]
Inducers						
Methyl 1-thio-β-D-galactoside	2×10^{-4}	$(1.3 \pm 0.3) \times 10^{-1}$	$(3.3 \pm 1.1) \times 10^2$	3.4×10^2	6.5×10^2	1.7×10^{-2}
Isopropyl β-D-galactoside						$(1.07 \pm 0.01) \times 10^{-2}$
Isopropyl 1-thio-β-D-galactoside	2×10^{-4}	$(2.0 \pm 0.4) \times 10^{-1}$	$(5.0 \pm 1.3) \times 10^3$	2.4×10^2	1×10^3	$(1.1 \pm 0.2) \times 10^{-2}$
p-Aminophenyl 1-thio-β-D-galactoside						$(1.1 \pm 0.1) \times 10^{-2}$
Galactose						$(9.2 \pm 0.3) \times 10^{-3}$
Melibiose	2×10^{-4}	$(1.2 \pm 0.3) \times 10^{-1}$	$(7.7 \pm 2.4) \times 10$	1.3×10^2	6×10^2	
Allolactose						1.4×10^{-2}
Anti-inducers[b]						
Phenyl β-D-galactoside	$(3.4 \pm 0.1) \times 10^{-4}$	$(1.9 \pm 0.3) \times 10^{-4}$	$(6.7 \pm 4.5) \times 10$	1.6×10	5.6×10^{-1}	
o-Nitrophenyl β-D-fucoside[c]	$(4.2 \pm 0.1) \times 10^{-4}$	$(1.4 \pm 0.1) \times 10^{-4}$	$(4.0 \pm 0.2) \times 10^3$	1.7	3.3×10^{-1}	
Glucose[c]	$(4.1 \pm 0.1) \times 10^{-4}$	$(2.0 \pm 0.3) \times 10^{-4}$	$(5.3 \pm 3.0) \times 10$	3.0×10^{-1}	4.9×10^{-1}	
Lactose[c]	$(4.1 \pm 0.1) \times 10^{-4}$	$(7.5 \pm 1.5) \times 10^{-5}$	$(2.2 \pm 0.3) \times 10$	1.4×10^{-1}	1.8×10^{-1}	

[a] Values calculated by linear regression of the data to 70% confidence. [b] Rate constants of dissociation for anti-inducers were measured in BB, $I = 0.1$ *M*. [c] Data published previously (Jobe and Bourgeois, 1973).

ly the same relative affinity for free *lac* repressor as compared to repressor bound to operator DNA, the affinity of inducer for repressor being about 200-fold greater than that for repressor–operator complex.

Kinetic experiments with the wild-type Q repressor in the presence of high concentrations of inducer are difficult, because of the very short half-lives of dissociation. In order to verify that the effected rate constant k_{b1} is identical for a variety of inducing ligands, experiments at saturating concentrations of inducer were carried out using X86 repressor (Chamness and Wilson, 1970), which has a 35-fold increased affinity for operator DNA (Jobe and Bourgeois, 1972b). Under standard conditions, the X86 repressor–operator complex decomposes with a spontaneous rate constant $^0k_{b1} \simeq 6 \times 10^{-6}$ sec^{-1} in the absence of inducing ligand and with an effected rate constant $k_{b1} = 3.9 \times 10^{-3}$ sec^{-1} at saturating concentrations of IPTG. Thus, direct measurement of k_{b1}, without extrapolation of the data for k_{bapp} as a function of ligand concentration, is possible. Representative inducers, having aliphatic and aromatic substituents, as well as some natural sugars, were tested with X86 repressor; the effected rate constants of dissociation k_{b1} are registered in Table III, column 2. Again, within experimental error, k_{b1} is the same for the inducers studied.

Neutral Ligands. In the process of categorizing sugars as effecting ligands of the *lac* repressor, one compound, *o*-nitrophenyl β-D-galactoside (ONPG), was found to bind to repressor protein but to exert no effect on the interaction of repressor and operator DNA. The association constant for the binding of ONPG to repressor, as determined by equilibrium dialysis using the Lineweaver–Burk technique, is $K_2 = 9.2 \times 10^3$ M^{-1}. ONPG is a competitive inhibitor of the binding of [^{14}C]IPTG, as evidenced by a linear double reciprocal plot of the data (not shown) with constant intercept on the ordinate.

In experiments to determine the effect of ligand on the interaction of repressor and operator, no difference was seen in the equilibrium formation of repressor–operator complex in the presence or absence of 0.03 *M* ONPG (the highest concentration possible, due to limits of solubility), and no change in the rate constant of dissociation of repressor–operator complex was detected at this concentration of ONPG, 300-fold above the equilibrium dissociation constant for binding to repressor.

Anti-inducers

(*a*) *Equilibrium Binding.* The association constants for the binding of anti-inducing ligands to *lac* repressor as determined in equilibrium dialysis experiments by competition against [^{14}C]IPTG are given in the first column of Table I. The double reciprocal plots (not shown) of the equilibrium dialysis data were linear, and the intercept on the ordinate constant, suggesting that the anti-inducers are competitive inhibitors of the [^{14}C]IPTG binding. We have not been able to measure the binding of labeled anti-inducing ligand to repressor by equilibrium dialysis at this time, because of technical difficulties associated with the low affinities.

(*b*) *Kinetic Studies with Anti-inducers.* The dependence upon ligand concentration of the specific rate constant of dissociation of repressor–operator complex has been examined for the anti-inducers phenyl β-D-galactoside, ONPF, glucose, and lactose. The experiments were performed in BB at ionic strength $I = 0.1$ *M*, where the spontaneous rate constant of dissociation $^0k_{b1}$ is faster, 4×10^{-4} sec^{-1} compared to 2×10^{-4} sec^{-1} at $I = 0.05$ *M*, in order to allow measurement of the longer half-lives of the decomposition reaction at saturating concentrations of anti-inducer over a convenient time period. From the conclusions regarding the effect of ionic strength upon induction described in the section on IPTG, it is presumed that the values of the effected rate constant k_{b1} have the same dependence on ionic strength as those of $^0k_{b1}$ and that the values of K_3 are independent of ionic strength. The data for the half-lives of dissociation of repressor–operator complex as a function of concentration of anti-inducing ligand for ONPF, glucose, and lactose are shown in an earlier publication (Jobe and Bourgeois, 1973). For anti-inducers, the effected rate constant k_{1b} was determined by measurement of the rate constant of dissociation at saturating concentrations of ligand. The apparent equilibrium association constant K_3 for the binding of anti-inducer to repressor–operator complex was extracted from the plot of k_{bapp} vs. [L]. The values of k_{b1} and K_3 for the four above-mentioned anti-inducers are given in Table III, column 1. For reference, the values of the control in the absence of ligand, $^0k_{b1}$ at $I = 0.1$ *M*, are also recorded in column 1. The ratios of the association constant K_2 for the binding of anti-inducer to repressor, as

measured by equilibrium dialysis, to K_3 are tabulated in column 1.

Several aspects of these results should be noted. First, for lactose the value of the effected rate constant k_{bl} is significantly different from those for the other anti-inducers. Second, the ratio K_2/K_3 varies considerably, two compounds binding with greater affinity to repressor–operator complex and two with greater affinity to repressor. And lastly, it is emphasized that the magnitude of the decrease in the rate constant of dissociation at saturating concentrations of ligand is at most fivefold.

Discussion

The association constants K_2 for the binding of various sugar molecules to repressor ($R + L \rightleftharpoons RL$) have been determined in equilibrium dialysis experiments. Since no homotropic interactions between the ligand-binding sites of free repressor were detected for inducing ligands, we conclude, in agreement with previous reports (Gilbert and Müller-Hill, 1966), that the sites for inducing ligand are identical, independent sites. And since no heterotropic interactions in the binding of ^{14}C-labeled IPTG and anti-inducing ligands were observed, we suggest that inducers and anti-inducers bind to the same site. This latter inference is supported by biochemical evidence that in a mutated i^s repressor protein the IPTG- and ONPF-binding sites overlap (Jobe et al., 1972). The effected rate constants k_{bl} of dissociation of repressor–operator complex at saturating concentrations of ligand ($RL + O \rightleftharpoons ORL$) have been measured for inducing and anti-inducing ligands, and the association constants for the binding of repressor–ligand complex to operator DNA have been evaluated. In the case of inducing ligands, the effected rate constants converge to a single value within the limits of experimental error: $k_{bl} = 0.2$ sec^{-1}, corresponding to a half-life of 2.4 sec. Thus, all inducers destabilize repressor–operator complex to the same extent, about 1000-fold in the standard buffer; the magnitude of destabilization is sensitive to Mg^{2+} ion concentration, but not to ionic strength, pH, and temperature. This result, in conjunction with the results of the qualitative equilibrium test for induction, implies that there is a single mechanism for induction and that all inducers activate this process in a similar manner. Anti-inducers stabilize repressor–operator complex at most fivefold, and the value of k_{bl} for lactose differs appreciably from the others. The apparent association constants K_3 for the binding of effecting ligands to repressor–operator complex ($RO + L \rightleftharpoons ORL$) have been ascertained from the functional dependence of the rate constant of dissociation of repressor–operator complex upon ligand concentration. For those effecting ligands for which complete kinetic studies exist, the ratio of the affinity of effecting ligand for the two forms of repressor protein, free repressor and repressor bound to operator, is computed. The results, with the exception noted below, are qualitatively in accord with the predictions from simple thermodynamic considerations. That is, inducing ligands must have greater affinity for free repressor than for repressor–operator complex, and conversely, for anti-inducing ligands. For the inducers studied in detail, the equilibrium constant for binding to repressor is larger by at least two orders of magnitude than the equilibrium constant for binding to repressor–operator complex. Since we surmise that all inducers interact with repressor—operator complex by the same mechanism, and we have a measure κ of the relative potency of the various inducers in the equilibrium test for induction (Table I), we can estimate the association constants for binding to repressor–operator complex of the remaining inducers. We conclude that all the inducing ligands bind with greater affinity to free repressor than to repressor–operator complex. For the anti-inducers, the results are mixed. The two natural sugars, lactose and glucose, satisfy the criterion of anti-inducing ligands, binding with greater affinity to repressor–operator complex than to free repressor. The two phenyl sugars, ONPF and phenyl β-D-galactoside, exhibit anomalous behavior in the sense that they stabilize repressor–operator complex, yet seem to bind with greater affinity to free repressor than to repressor–operator complex. At present, we proffer no explanation for this result that is not in keeping with theory.

Because the repressor is a tetrameric protein, because the in vivo induction curves are sigmoidal, and because the elegant theory of allostery was developed with the *lac* operon in mind, it was anticipated that cooperative effects would be seen, if not in the binding of inducer to free repressor, at least in its interaction with repressor–operator complex. By comparing theoretical curves based on simple models of the induction process to the experimental plots of the apparent specific rate constant of dissociation of repressor–operator complex as a function of the concentration of effecting ligand (Figure 2), we can reach some conclusions regarding possible mechanisms of induction. In the Appendix, the mathematical formalism is developed for two rudimentary models: an extreme cooperative model, in which binding of a specified inducer molecule to repressor–operator complex causes a concerted allosteric transformation in the repressor tetramer, resulting in full induction in a single step; and a noncooperative model, in which N subunits interact with operator and each inducer molecule binding to repressor–operator complex causes a separate conformational transition in that repressor subunit, resulting in partial induction at each step. Since the observed dependence of the rate constant of dissociation upon concentration of effecting ligand is hyperbolic, our data permit us to rule out highly cooperative mechanisms of induction having positive interactions between the ligand-binding sites. Presumably, the change in affinity of repressor for operator DNA caused by effecting ligands is mediated through a conformational alteration in the protein. A change in the conformation of free repressor protein upon binding of inducer IPTG, but not upon binding of anti-inducers, has been detected by a number of investigators (Laiken et al., 1972; Ohshima et al., 1972; Matthews et al., 1973; M. D. Barkley, unpublished data, 1972).

A model in which repressor–operator complex has one apparent low-affinity site for inducer is the simplest model satisfying the experimental results. But, on the basis of our measurements which do not go below 10^{-6} M IPTG, we cannot distinguish between this case and the other models showing very weak cooperativity. For the X86 repressor, the curve depicting the dependence of the apparent rate constant of dissociation upon IPTG concentration is definitely sigmoid at low concentrations of inducer (Pfahl, 1974). In the case of the wild-type repressor, a small degree of curvature can be seen at IPTG concentrations between 10^{-7} and 10^{-6} M (Pfahl, unpublished data, 1974). The evidence on the molecular shape and subunit structure of the repressor protein (Steitz et al., 1974) suggests that more than one subunit may interact with operator DNA; presumably, these multiple interactions would be sensitive to inducer. It is an interesting consequence of the noncooperative model that, despite the absence of concerted interactions between

protein subunits, some cooperativity with respect to operator binding arises from the fact that the N subunits are bound to a single linear DNA polymer. The ratio K_2/K_3 of affinity of effecting ligand for free repressor to that for repressor bound to operator (Table III, column 1) and the ratio ${}^0K_1/K_1$ of affinity of operator for free repressor to that for repressor bound to ligand (Table III, column 1) have known relationships, depending upon the model. If there were one apparent site for effecting ligand on repressor–operator complex, then the values of the ratios K_2/K_3 and ${}^0K_1/K_1$ should be equal. All things considered, the agreement is not unreasonable. Yet the discrepancy is larger than the estimated errors: there is at least a factor of two that we cannot explain. For the noncooperative model with $N = 2$, the ratio K_2/K_3 for IPTG becomes 1.1×10^2 and should equal $({}^0K_1/K_1)^{1/2} = 32$. Here again, the relative difference is about the same, although in the opposite direction. If we note that for IPTG the value of K_2 in phosphate buffer is about twofold greater than the reported value in Tris buffer containing Mg^{2+} (Gilbert and Müller-Hill, 1966) and account for this in computing K_2/K_3, then the fit becomes more disparate for the case of $N = 1$ and is quite good for the case of $N = 2$. In sum, by numerology we really cannot distinguish between $N = 1$ and $N = 2$. Our preference for $N = 1$ is dictated by the shape of the curve (Figure 2) and the convenience of the analysis of the data.

At the inception of this work, we had hoped by quantitating the binding of a wide variety of effecting ligands to repressor protein and to repressor–operator complex to be able to point to some chemical features of the sugar molecule which determine its relative affinity for repressor and the direction of its effect on the stability of repressor–operator complex. All the compounds investigated can be assigned to one of three classes: inducing, neutral, and anti-inducing ligands. The majority of glycosides which bind to *lac* repressor are inducers. No new anti-inducers were discovered, an indication that the ability to stabilize repressor–operator complex is a special function. No compounds exhibited so-called "paradoxical" behavior, such as destabilizing repressor–operator complex at one concentration of ligand and stabilizing it at another. Of those sugar molecules reported to act paradoxically in vivo (Williams and Paigen, 1966), three are inducers: *p*-aminophenyl β-D-galactoside, *p*-aminophenyl 1-thio-β-D-galactoside, and D-fucose, and one is an anti-inducer: phenyl β-D-galactoside. However, we find one member, ONPG, of a new class of neutral ligands, which bind to free repressor but do not alter the repressor–operator interaction. The chemical basis of the interaction of ligand with repressor remains completely obscure. The substitution of oxygen by sulfur in the glycosidic linkage does not lead to a consistent change in the affinity of ligand for repressor. The simple rules proposed as requisite characteristics for anti-inducers: the glycone is 1-*O*-β-D-galactopyranoside modified at the C-6 position, the C-1 residue is ortho-substituted phenol, and restricted rotation of the ortho-substituted benzyl ring be a common property (Müller-Hill et al., 1964) are abolished by the fact that phenyl β-D-galactoside, glucose, and lactose are anti-inducers and ONPG is not. We conclude that binding studies alone are not sufficient to elucidate those features of the sugar molecule important for interaction with free repressor or for distinguishing between inducers and anti-inducers.

Appendix

Derivation of Rate Expression. Small ligands interacting with the *lac* repressor protein alter the rate of dissociation of repressor–operator complex. In this section, we derive expressions for the specific rate constant of dissociation of repressor–operator complex in the presence of effecting ligands. First, we present the general kinetic equations for the case of N sites for ligand per repressor molecule. We then show the results of sample calculations, assuming simple models for the interaction of effecting ligand with repressor–operator complex.

Since one oligomeric repressor molecule R binds to one operator DNA site O, the expressions describing the binding of N ligand molecules L to repressor protein in the presence of operator DNA are

$$\begin{array}{lcccl}
 & \mathrm{R} + \mathrm{O} & \underset{{}^0k_{b1}}{\overset{{}^0k_{f1}}{\rightleftharpoons}} & \mathrm{RO} & (1.0) \\
 & + & & + & \\
 & \mathrm{L} & & \mathrm{L} & \\
(2.1) & \Big\updownarrow {}^1K_2 & & \Big\updownarrow {}^1K_3 & (3.1) \\
 & \mathrm{RL} + \mathrm{O} & \underset{{}^1k_{b1}}{\overset{{}^1k_{f1}}{\rightleftharpoons}} & \mathrm{ORL} & (1.1) \\
 & \mathrm{RL}_{i-1} + \mathrm{O} & \underset{{}^{i-1}k_{b1}}{\overset{{}^{i-1}k_{f1}}{\rightleftharpoons}} & \mathrm{ORL}_{i-1} & (1.i\text{-}1) \\
 & + & & + & \\
 & \mathrm{L} & & \mathrm{L} & \\
(2.i) & \Big\updownarrow {}^iK_2 & & \Big\updownarrow {}^iK_3 & (3.i) \\
 & \mathrm{RL}_i + \mathrm{O} & \underset{{}^ik_{b1}}{\overset{{}^ik_{f1}}{\rightleftharpoons}} & \mathrm{ORL}_i & (1.i) \\
 & \mathrm{RL}_N + \mathrm{O} & \underset{{}^Nk_{b1}}{\overset{{}^Nk_{f1}}{\rightleftharpoons}} & \mathrm{ORL}_N & (1.N)
\end{array}$$

where the ${}^ik_{f1}$ and ${}^ik_{b1}$, $i = 0, 1, \ldots, N$, are the specific rate constants of association and dissociation, respectively, for reaction 1.*i*, the binding of repressor bearing i ligands and operator; ${}^iK_2$, $i = 1, \ldots, N$, is the equilibrium association constant for reaction 2.*i*, the binding of the ith ligand and repressor; and ${}^iK_3$, $i = 1, \ldots, N$, is the equilibrium association constant for reaction 3.*i*, the binding of the ith ligand and repressor–operator complex. The equilibrium association constant governing reaction 1.*i* is

$${}^iK_1 = \frac{{}^ik_{f1}}{{}^ik_{b1}} = \begin{cases} \dfrac{[\mathrm{RO}]}{[\mathrm{R}][\mathrm{O}]} & i = 0, \\ \dfrac{[\mathrm{ORL}_i]}{[\mathrm{RL}_i][\mathrm{O}]} & i = 1,\ldots,N \end{cases} \qquad (3.i)$$

Since the binding reactions 1.*i*-1, 2.*i*, 1.*i*, and 3.*i* comprise a closed path, the equilibrium constants ${}^{i-1}K_1$, ${}^iK_2$, ${}^iK_1$, and ${}^iK_3$ necessarily obey the relationship

$$\frac{{}^{i-1}K_1}{{}^iK_1} = \frac{{}^iK_2}{{}^iK_3} \qquad i = 1,\ldots,N \qquad (4.i)$$

In kinetic experiments using the membrane filter technique, radioactively labeled operator DNA bound to repressor protein is monitored. Define O^* to be the sum of all the radioactive species trapped on the filters, that is

$$O^* = [\mathrm{RO}] + \sum_{i=1}^{N} [\mathrm{ORL}_i] \qquad (5)$$

The equation for the rate of disappearance of O^* is

$$\frac{-\mathrm{d}O^*}{\mathrm{d}t} = {}^0k_{b1}[\mathrm{RO}] - {}^0k_{f1}[\mathrm{R}][\mathrm{O}] + \sum_{i=1}^{N} ({}^ik_{b1}[\mathrm{ORL}_i] - {}^ik_{f1}[\mathrm{RL}_i][\mathrm{O}]) \qquad (6)$$

Since the affinity of repressor for effecting ligand is at least 10^7-fold less than the affinity of repressor for operator DNA, the experiments are carried out under conditions where [L] $\gg$ [R], [O]. We assume that the equilibria of reactions 2.*i* and 3.*i* are attained rapidly compared to those of reactions 1.*i*, that is, that effecting ligand is in equilibrium with repressor and with repressor-operator complex at all times. Thus, we may compute the concentrations of RL_i and of ORL_i from the appropriate equilibrium expressions

$$[RL_i] = \left(\prod_{j=1}^{i} {}^{j}K_2\right)[R][L]^i \quad i = 1,\ldots,N \quad (7.i)$$

$$[ORL_i] = \left(\prod_{j=1}^{i} {}^{j}K_3\right)[RO][L]^i \quad i = 1,\ldots,N \quad (8.i)$$

Substitution of eq 7.*i* and 8.*i* into eq 5 and 6 and combination of the resulting equations for O^* and $-dO^*/dt$ yield an expression for the rate of disappearance of repressor-operator complexes in the presence of effecting ligand as determined by membrane filtration

$$\frac{-dO^*}{dt} = \frac{O^*\left\{{}^{0}k_{b1} + \sum_{i=1}^{N} {}^{i}k_{b1}\left(\prod_{j=1}^{i} {}^{j}K_3\right)[L]^i\right\}}{1 + \sum_{i=1}^{N}\left(\prod_{j=1}^{i} {}^{j}K_3\right)[L]^i} - [R][O]\left\{{}^{0}k_{f1} + \sum_{i=1}^{N} {}^{i}k_{f1}\left(\prod_{j=1}^{i} {}^{j}K_2\right)[L]^i\right\} \quad (9)$$

In order to measure the rate of dissociation of repressor-operator complexes, at time $t = 0$ a large excess of unlabeled operator DNA is added to a previously equilibrated mixture of repressor and labeled operator DNA. For the initial part of the reaction, [R] $\rightarrow$ 0; the second term in eq 9 is negligible compared to the first term until a new equilibrium is obtained.

Thus, to a good approximation

$$\frac{-dO^*}{dt} = k_{bapp}O^* \quad (10)$$

where the apparent specific rate constant of dissociation is defined as

$$k_{bapp} = \frac{{}^{0}k_{b1} + \sum_{i=1}^{N} {}^{i}k_{b1}\left(\prod_{j=1}^{i} {}^{j}K_3\right)[L]^i}{1 + \sum_{i=1}^{N}\left(\prod_{j=1}^{i} {}^{j}K_3\right)[L]^i} \quad (11)$$

Equation 11 is a rather complicated, general expression for the rate constant for the dissociation of repressor-operator complex as a function of the concentration of effecting ligand, and as such is not readily interpretable. It involves a spectrum of rate constants ${}^{0}k_{b1}, \ldots, {}^{N}k_{b1}$, with each species ORL_i dissociating to RL_i and O with a different rate constant ${}^{i}k_{b1}$. However, some insight may be gained by examining the behavior of this equation at the extremes of low and high ligand concentrations. As L $\rightarrow$ 0, $k_{bapp} \rightarrow {}^{0}k_{b1}$ as required. On the other hand, as L $\rightarrow \infty$, $k_{bapp} \rightarrow {}^{N}k_{b1}$; that is, k_{bapp} approaches a limiting value. The effect of ligand on the rate constant of dissociation saturates at high concentrations of ligand and k_{bapp} becomes independent of [L], as expected from physical arguments. Rewriting eq 11 in inverse form

$$\frac{1}{k_{bapp} - {}^{0}k_{b1}} = \frac{1 + \sum_{i=1}^{N}\left(\prod_{j=1}^{i} {}^{j}K_3\right)[L]^i}{\sum_{i=1}^{N}({}^{i}k_{b1} - {}^{0}k_{b1})\left(\prod_{j=1}^{i} {}^{j}K_3\right)[L]^i}$$

and considering [L] very large, give the following relationship

$$\frac{1}{k_{bapp} - {}^{0}k_{b1}} \rightarrow \frac{1}{({}^{N}k_{b1} - {}^{0}k_{b1})}\left\{\frac{1}{{}^{N}K_3[L]} + 1\right\} \quad (12)$$

Thus, a double reciprocal plot of $1/(k_{bapp} - {}^{0}k_{b1})$ vs. $1/[L]$ becomes linear as $1/[L] \rightarrow 0$; the line has a slope of $1/({}^{N}k_{b1} - {}^{0}k_{b1}){}^{N}K_3$ and an intercept of $1/({}^{N}k_{b1} - {}^{0}k_{b1})$. This plot may be used to determine the value of the rate constant ${}^{N}k_{b1}$ at saturating concentrations of ligand. So far, no assumptions regarding the mechanism of induction have been introduced into the equations, and the value of ${}^{N}k_{b1}$ obtained by this method is invariant of model.

For the *lac* repressor, an oligomeric protein composed of four identical subunits, we examine two simple mechanisms for the allosteric transition supposed to occur upon induction. The first model, the extreme cooperative model, is a single-state model with respect to binding to operator DNA. The entire protein molecule can exist in either one of two conformational states, the operator-binding or the inducer-binding form. The change in conformation occurs in concert in all the subunits. The second model, the noncooperative model, is a multi-state model with respect to binding to operator. Each protein subunit interacting with operator DNA can independently undergo a conformational transition.

In the case of the extreme cooperative model, assume there are two rate constants possible for the dissociation of a given species ORL_i into RL_i and O: the spontaneous rate constant ${}^{0}k_{b1}$, the rate constant for the dissociation of RO in the absence of ligand, or the effected rate constant k_{b1}. The induction process is visualized as follows. Ligand binds to repressor-operator complex with no change in the rate of dissociation from the spontaneous rate, until the *l*th effecting molecule binds and triggers a conformational transition. Then the repressor-operator complex ORL_l dissociates with the effected rate constant. Binding of additional ligand causes no further change in the rate of dissociation. Operationally, if the *l*th molecule effects

$${}^{i}k_{b1} = \begin{cases} {}^{0}k_{b1} & i < l \\ k_{b1} & i \geq l \end{cases} \quad \text{for } i = 1,\ldots,N \quad (13.i)$$

and

$$\frac{{}^{i-1}K_1}{{}^{i}K_1} = \begin{cases} {}^{i}k_{b1}/{}^{0}k_{b1} & i \neq l \\ & i = l \end{cases} \quad (14.i)$$

since the rate of association of repressor-operator complex is the same in the presence and absence of effecting ligand. By coupling eq 4.*i* and the expression (see Tanford, 1961) relating the ${}^{i}K_2$'s for the binding of ligand to identical, noninteracting sites on free repressor to a single equilibrium association constant K_2, with eq 14.*i*, formulas for the ${}^{i}K_3$'s are obtained.

$${}^{i}K_3 = \begin{cases} {}^{i}K_2 = \dfrac{(N - i + 1)}{i}K_2 & i \neq l \\ \dfrac{{}^{0}k_{b1}}{k_{b1}}\,{}^{i}K_2 = \dfrac{{}^{0}k_{b1}(N - l + 1)K_2}{k_{b1}l} & i = l \end{cases} \quad \text{for } i = 1,\ldots,N \quad (15.i)$$

Substitution of eq 13.*i* and 15.*i* into eq 11 and execution of the indicated mathematical manipulations give an expression for the apparent specific rate constant for the extreme cooperative model, where the *l*th ligand bound induces the allosteric transformation

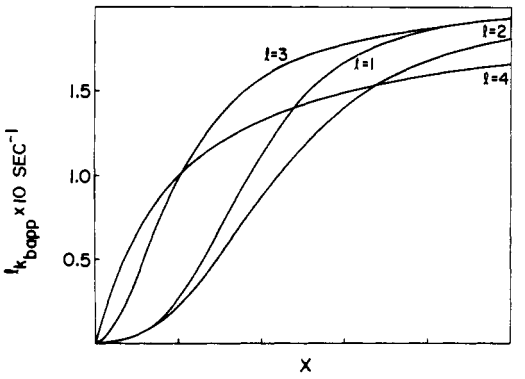

FIGURE 3: Extreme cooperative model. Curves are generated from eq 16 for $N = 4$, ${}^0k_{b1} = 2 \times 10^{-4}$ sec^{-1}, $k_{b1} = 2 \times 10^{-1}$ sec^{-1}; the values of l are indicated. The scaling factor $X = {}^lK_3[L]$; X ranges from 0 to 0.05 for $l = 1$ and 2, to 0.25 for $l = 3$, to 5 for $l = 4$.

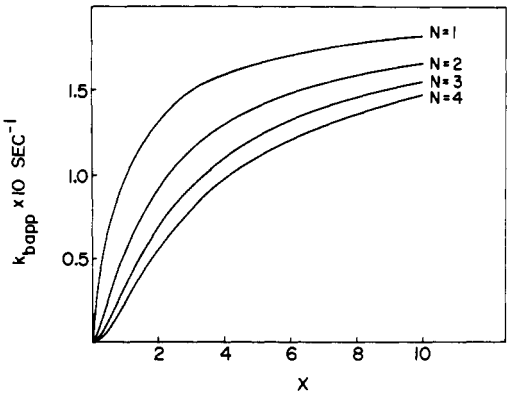

FIGURE 4: Noncooperative model. Curves are generated from eq 20 for ${}^0k_{b1} = 2 \times 10^{-4}$ sec^{-1}, $k_{b1} = 2 \times 10^{-1}$ sec^{-1}; the values of N are indicated. The scaling factor $X = K_3[L]$.

$$ {}^lk_{bapp} = \frac{k_{b1}\left\{1 + \frac{k_{b1}}{{}^0k_{b1}}\frac{K_3{}^l[L]l}{(N - l + 1)}\right\}^N}{\left\{\frac{k_{b1}}{{}^0k_{b1}} - 1\right\}\left\{1 + \sum_{i=1}^{l-1}\frac{N!}{(N-i)!\,i!}\frac{k_{b1}}{{}^0k_{b1}}\frac{K_3{}^l[L]^i l}{(N - l + 1)}\right\} + \left\{1 + \frac{k_{b1}}{{}^0k_{b1}}\frac{K_3{}^l[L]l}{(N - l + 1)}\right\}^N} \quad (16) $$

Note that in the limit $[L] \rightarrow \infty$, ${}^lk_{bapp} \rightarrow k_{b1}$, for $l = 1, \ldots, N$, and k_{b1} may be identified as the saturated specific rate constant ${}^Nk_{b1}$.

The simplest example of the noncooperative model presumes that N repressor subunits, each bearing a site for effecting ligand, participate in the binding of operator DNA and contribute equally to the interaction. In this situation, binding of ligand to an individual repressor subunit effects a conformational transition in that subunit, altering the affinity of repressor for operator by a factor corresponding to the Nth root of the overall change in the association constant ${}^0K_1/{}^NK_1$, that is

$$ \frac{{}^{i-1}K_1}{{}^iK_1} = \left(\frac{{}^Nk_{b1}}{{}^0k_{b1}}\right)^{1/N} \qquad i = 1, \ldots, N \quad (17.i) $$

and

$$ {}^ik_{b1} = \left(\frac{{}^Nk_{b1}}{{}^0k_{b1}}\right)^{i/N}{}^0k_{b1} \qquad i = 1, \ldots, N \quad (18.i) $$

The sites for ligand on repressor-operator complex are likewise identical and independent sites, and the ${}^iK_3$'s are related to a single equilibrium association constant K_3

$$ {}^iK_3 = \frac{(N - i + 1)}{i}K_3 \qquad i = 1, \ldots, N \quad (19.i) $$

where necessarily

$$ K_3 = \left(\frac{{}^0k_{b1}}{{}^Nk_{b1}}\right)^{1/N}K_2 $$

Inserting eq 18.*i* and 19.*i* into eq 11 and performing the mathematical operations, we obtain an expression for the apparent specific rate constant for the noncooperative model

$$ k_{bapp} = \frac{{}^0k_{b1}\left\{1 + \left(\frac{{}^Nk_{b1}}{{}^0k_{b1}}\right)^{1/N}K_3[L]\right\}^N}{(1 + K_3[L]^N} \quad (20) $$

The results of sample calculations of the extreme cooperative and the noncooperative models are presented in Figures 3 and 4, respectively, for an inducing ligand. In Figure 3, ${}^lk_{bapp}$ is computed from eq 16 for $N = 4$; the values of l are indicated on the curves, and the scaling parameter $X = {}^lK_3[L]$. In Figure 4, k_{bapp} is computed from eq 20; the values of N are indicated on the curves, and the scaling parameter $X = K_3[L]$. Obviously, for the case of $N = 1$, the two models are identical. The value of X on the theoretical curve which corresponds to half the possible change in rate constant, that is, to

$$ k^*{}_{bapp} = {}^1/_2|{}^Nk_{b1} - {}^0k_{b1}| \quad (21) $$

is called X^*. For $N = 1$, $X^* = 1$.

In the extreme cooperative model, the plots of ${}^lk_{bapp}$ vs. X, as evidenced in Figure 3, are S-shaped for all $l < N$ and hyperbolic for $l = N$, the degree of sigmoidicity decreasing with increasing l. The values of $X^* \leq 1$, and vary with l over a substantial range; in the example of $N = 4$, X^* increases ~50-fold as $l \rightarrow 1$ to 4. The pronounced sigmoidal behavior of ${}^lk_{bapp}$ as a function of X is displayed as upward curvature in a double reciprocal plot of $1/({}^lk_{bapp} - {}^0k_{b1})$ vs. $1/X$. The two end cases of $l = 1$ and $l = N$ deserve special comment. The case of $l = 1$, in which the first inducing ligand binds to repressor-operator complex, simultaneously causing induction and promoting the affinity of the sites for inducer to the value characteristic of free repressor, is closest to the classical allosteric model (Monod et al., 1965). Here there is positive cooperativity among the ligand-binding sites of repressor bound to operator DNA. The case of $l = N$, in which the first $(N - 1)$ inducer molecules bind to repressor-operator complex with an affinity identical with that for free repressor and the last molecule binds with lower affinity, inducing the conformational transition, represents negative cooperativity among the ligand-binding sites on repressor bound to operator. Moreover, for inducing ligands, ${}^Nk_{b1} \gg {}^0k_{b1}$, the plot of k_{bapp} vs. X coincides with that for the case of $N = 1$. This result is apparent by reasoning that, if the affinities of the two kinds of sites are widely separated, the $(N - 1)$ high-affinity sites are saturated at very low concentrations of inducing ligand, and the repressor-operator complex behaves at the higher ligand concentrations, where induction occurs, as if it had only the single low-affinity site for inducer.

In the noncooperative model, the plots of k_{bapp} vs. X, as shown in Figure 4, are hyperbolic for $N = 1$ and approximately hyperbolic for $N > 1$, with some curvature at small X; the degree of curvature increases as N increases. The

values of $X^* \geq 1$, increasing slightly with N. Again, the slight sigmoid character of k_{bapp} at small X is manifest in upward curvature of the double reciprocal plot at larger values of $1/X$. In this model, a kind of weak cooperativity in the induction process develops from the fact that the binding of each inducing ligand reduces the affinity of repressor for operator by a multiplicative factor.

To summarize, we have a detailed understanding of two simple models for induction, the extreme cooperative model and the noncooperative model, which may be advanced in order to interpret the observed dependence of the apparent specific rate constant of dissociation of repressor–operator complex on concentrations of effecting ligand. We may reach some qualitative conclusions about the mechanism of induction on the basis of the shape of the experimental curves. And we can establish a quantitative value for K_3, the association constant for the binding of effecting ligand to repressor–operator complex, by fitting the theoretical curves to the experimental data. It should be clear from the preceding discussion that the value of K_3 is sensitive to the model chosen.

Acknowledgments

We thank Dr. Raymond J. Kelleher and Professor Bruno H. Zimm for fecund discussions, and Ms. J. Roberts for excellent assistance with kinetic experiments. We acknowledge the contributions of Dr. Magnus Pfahl in the form of lively debate and of generous sharing of his unpublished data.

References

Boos, W., Schaedel, P., and Wallenfels, K. (1967), *Eur. J. Biochem. 1,* 382.

Bourgeois, S., and Riggs, A. D. (1970), *Biophys. Biochem. Res. Commun. 38,* 348.

Chamness, G. C., and Wilson, C. D. (1970), *J. Mol. Biol. 53,* 561.

Davoll, J., Lythgoe, B., and Todd, A. R. (1948), *J. Chem. Soc.,* 967.

Gilbert, W., and Müller-Hill, B. (1966), *Proc. Natl. Acad. Sci. U.S.A. 56,* 1891.

Hayes, D. H., and Todd, A. R. (1950), *J. Chem. Soc.,* 303.

Helferich, B., and Sparmberg, G. (1933), *Ber. 66,* 806.

Jobe, A., and Bourgeois, S. (1972a), *J. Mol. Biol. 69,* 397.

Jobe, A., and Bourgeois, S. (1972b), *J. Mol. Biol. 72,* 139.

Jobe, A., and Bourgeois, S. (1973), *J. Mol. Biol. 75,* 303.

Jobe, A., Riggs, A. D., and Bourgeois, S. (1972), *J. Mol. Biol. 64,* 181.

Laiken, S. L., Gross, C. A., and von Hippel, P. H. (1972), *J. Mol. Biol. 66,* 143.

Lin, S.-Y., and Riggs, A. D. (1972), *J. Mol. Biol. 72,* 671.

Lineweaver, H., and Burk, D. (1934), *J. Am. Chem. Soc. 56,* 658.

Matthews, K. S., Matthews, H. R., Thielmann, H. W., and Jardetzky, O. (1973), *Biochim. Biophys. Acta 295,* 159.

Miller, J. H., Beckwith, J., and Müller-Hill, B. (1968), *Nature (London) 220,* 1287.

Monod, J., Wyman, J., and Changeux, J.-P. (1965), *J. Mol. Biol. 12,* 88.

Monod, J., Cohen-Bazire, G., and Cohn, M. (1951), *Biochim. Biophys. Acta 7,* 585.

Müller-Hill, B., Rickenberg, H. V., and Wallenfels, K. (1964), *J. Mol. Biol. 10,* 303.

Ohshima, Y., Matsurra, M., and Horiuchi, T. (1972), *Biochem. Biophys. Res. Commun. 47,* 1444.

Pfahl, M. (1974), *J. Mol. Biol.* (in press).

Riggs, A. D., Bourgeois, S., and Cohn, M. (1970a), *J. Mol. Biol. 53,* 401.

Riggs, A. D., Newby, R. F., and Bourgeois, S. (1970b), *J. Mol. Biol. 51,* 303.

Riggs, A. D., Suzuki, H., and Bourgeois, S. (1970c), *J. Mol. Biol 48,* 67.

Scatchard, G. (1949), *Ann. N.Y. Acad. Sci. 51,* 660.

Steitz, T. A., Richmond, T. J., Wise, D., and Engelman, D. (1974), *Proc. Natl. Acad. Sci. U.S.A. 71,* 593.

Tanford, C. (1961), Physical Chemistry of Macromolecules, New York, N.Y., Wiley, p 532.

Williams, B., and Paigen, K. (1966), *Biochem. Biophys. Res. Commun. 24,* 143.

Zubay, G. (1973), *Annu. Rev. Genet., 7,* 267.